Chinese Chemical Letters 35 (2024) 109170

Contents lists available at ScienceDirect

Chinese Chemical Letters

journal homepage: www.elsevier.com/locate/cclet

Redox responsive polymeric nanoparticles enhance the efficacy of cyclin dependent kinase 7 inhibitor for enhanced treatment of prostate cancer

Yiran Tao[a,b,c,1], Chunlei Dai[d,1], Zhaoxiang Xie[a,1], Xinru You[e], Kaiwen Li[a,*], Jun Wu[f,g,h,i,*], Hai Huang[a,f,g,j,*]

[a] Department of Urology, Sun Yat-sen Memorial Hospital, Sun Yat-sen University, Guangzhou 510120, China
[b] Department of Urology, The Sixth Affiliated Hospital, Sun Yat-sen University, Guangzhou 510120, China
[c] Biomedical Innovation Center, The Sixth Affiliated Hospital, Sun Yat-sen University, Guangzhou 510120, China
[d] School of Biomedical Engineering, Sun Yat-sen University, Shenzhen 518107, China
[e] Center for Nanomedicine and Department of Anesthesiology, Brigham and Women's Hospital, Harvard Medical School, Boston, MA 02115, United States
[f] Guangdong Provincial Key Laboratory of Malignant Tumor Epigenetics and Gene Regulation, Sun Yat-sen Memorial Hospital, Sun Yat-Sen University, Guangzhou 510120, China
[g] Department of Urology, The Sixth Affiliated Hospital of Guangzhou Medical University, Qingyuan People's Hospital, Qingyuan 511518, China
[h] Bioscience and Biomedical Engineering Thrust, The Hong Kong University of Science and Technology (Guangzhou), Guangzhou 511400, China
[i] Division of Life Science, The Hong Kong University of Science and Technology, Hong Kong, China
[j] Guangdong Provincial Clinical Research Center for Urological Diseases, Sun Yat-sen Memorial Hospital, Sun Yat-sen University, Guangzhou 510120, China

ARTICLE INFO

Article history:
Received 29 July 2023
Revised 26 September 2023
Accepted 5 October 2023
Available online 7 October 2023

Keywords:
Prostate cancer
Nanoparticles
CDK7
THZ1
THZ1@Cys8E NPs

ABSTRACT

Traditional therapies such as surgery and endocrine therapy no longer meet the clinical needs in prostate cancer treatment, and more effective treatments are urgently required. Recent studies have reported that targeted inhibition of the transcription factor cyclin dependent kinase 7 (CDK7) could effectively suppress prostate cancer progression. However, the toxicity of CDK7 inhibitors such as THZ1 is the main limitation of the clinical application. In this work, we synthesized Cys8E (C8E) nanoparticles (NPs) loaded with THZ1 (C8E@THZ1), a novel GSH-targeting and stimuli-responsive nano-delivery platform, and investigated its anti-tumor potential and biosafety properties. *In vitro*, C8E@THZ1 potently inhibited the proliferation and promoted the apoptosis of prostate cancer cells. On tumor-bearing mice, C8E@THZ1 inhibited tumors by up to 85%, while the damage of THZ1 to liver function was effectively avoided. These results confirmed that inhibition of CDK7 can effectively block the progression of prostate cancer, and that Cys8E NPs is a highly prospective delivery platform to promote the clinical application of CDK7 inhibitors.

Prostate cancer (PCa), next only to lung carcinoma, is viewed as the second most common cancer in global males and effects millions of men and accounts for about 7% of worldwide new cases of cancers among men. Here are more PCa patients emerging in high-income regions than low-income regions, whose prognosis varies are widely related with age, genetic background, ethnicity and stage of progression [1]. And among the Asian population, the incidence of PCa is lower than the Western, furthermore, but there is more metastasis and drug resistance cases [2]. As for the disease initiation, it is reported that the luminal prostate epithelial or basal cells might be origination of the tumor-initiating cells, and genetic mutation acts as a primary driver of PCa. Progression of prostate cancer, emerging in a large proportion of patients, is accompanied by incremental prostate specific antigen (PSA) level that is related to androgen receptor (AR) activity [1].

It is studied that AR is crucial for prostate cancer, meanwhile androgen deprivation therapy (ADT) is regarded as the standard therapeutic regimen for metastatic prostate cancer by removing testicular androgens through surgery or medicine castration [3]. Castration-resistant prostate cancer (CRPC), tumors recuring after ADT, might respond to therapeutic schedules that decrease androgen levels further through inhibiting androgen synthesis in adrenal gland and tumor cells such as abiraterone or agents directly antagonizing AR (*i.e.*, enzalutamide) [4]. As for most patients, ADT might bring an effective treating stage, but many of them would

* Corresponding authors.
E-mail addresses: likw6@mail.sysu.edu.cn (K. Li), junwuhkust@ust.hk (J. Wu), huangh9@mail.sysu.edu.cn (H. Huang).
[1] These authors contributed equally to this work.

https://doi.org/10.1016/j.cclet.2023.109170
1001-8417/

relapse and develop CRPC when the therapeutic effect of ADT fade away [5]. Nevertheless, the progression of metastatic CRPC could be postponed by the early application of androgen signaling inhibitors (ASI) combined with inhibitors of testicular androgens, and these joint uses of classical ADTs are gradually working as the subsequent mainstream treatment. Badly, most patients would relapse after initially responding to these therapeutic regimens. Here is an urgent need for further responses that might be maintained with drugs including poly(ADP-ribose) polymerase (PARP) inhibitors, immunotherapy, taxanes and so on but these agents work in a subset of tumors respectively [4].

The mediator complex subunit 1 (MED1) component of mediator (*i.e.*, TRAP220, PBP, or DRIP205) could bind to AR, a nuclear receptor, which could be promoted by the TAU1 site in the AR N-terminal domain. It is reported that protein kinase B (AKT), extracellular regulated protein kinases (ERK), and DNA-dependent protein kinase (DNA-PK) might mediate the phosphorylation of MED1 which facilitates MED1 to be involved in the Mediator complex and bind to AR. Moreover, MED1 phosphorylation at T1457, mediated by cyclin dependent kinase 7 (CDK7), that promotes its connection with AR. Importantly, it is said that increased MED1 phosphorylation is involved in enzalutamide resistance in CRPC xenograft models, and THZ1 (a covalent CDK7-specific inhibitor) could obstruct AR-mediated MED1 recruitment to chromatin. In conclusion, THZ1 could impair enzalutamide resistance and promote tumor regression in CRPC models that show a neoteric clinical treatment for advanced prostate cancer [6].

Poor targeting of conventional on tumor tissues agents is one of the crucial obstacles in cancer treatments that results in severe impairs on the normal parts. Here is a helpful method that nanoparticles work as an outstanding delivery system for facilitating the curative effect of diverse agents and enhancing the targeting function through intensified permeability and retention (EPR) effect. Besides, novel stimuli-responsive nanocarriers have been regarded as a resultful targeting method against tumors, as these nanoplatforms keep their unbroken structures under normal tissues, but broken and release loaded agents once entering the tumor microenvironment [7,8].

Based on previous research, our team has prepared an excellent polymer which named Cys8E. It has benign biocompatibility and sensitive glutathione (GSH)-responsiveness. Furthermore, here is enough drug loading capacity in Cys8E nanoparticles (NPs) and the tumor inhibitory ability of drug-loaded Cys8E NPs has been tested in other cancers [9]. In this article, we synthesized a new GSH-targeted nanoparticle Cys8E nanoparticles (C8E NPs) to carry THZ1 that named as THZ1@C8E NPs (C8E@THZ1). Both *in vitro* and *in vivo*, the C8E NPs could improve the aggregation of THZ1 and antitumor potential in PCa to a great extent. Besides, here are abundant drug loading efficiency, great stability and outstanding release capacity of loaded nanoparticles (Scheme 1).

For efficient loading and targeted delivery of THZ1 in PCa, we synthesized C8E polymer and the corresponding nanoparticles, C8E@THZ1. On the basis of the ^{1}H NMR spectrum, the exact chemical structure characteristics of C8E polymer was demonstrated (Fig. 1A). And the average size of C8E@THZ1 is 91.62 ± 2.58 nm with a narrow polydispersity index (PDI) (Figs. 1B and E). Additionally, the homogeneous and complete spherical morphology of the C8E@THZ1 (Fig. 1C) and C8E NPs (Fig. 1D) were displayed by the transmission electron microscope (TEM) images, which was consistent with the dynamic light scattering (DLS) results.

Next, the stability and drug release behavior are significant for the nanoparticles. Dispersed in phosphate buffered saline (PBS) containing 10% serum and PBS for 7 days, C8E NPs or C8E@THZ1 had a slight particle size change (90–110 nm) (Fig. 1F), indicating that the nanoparticles were stable. Under 20 mmol/L dithiothreitol (DTT) conditions, the cumulative release of THZ1 from C8E@THZ1

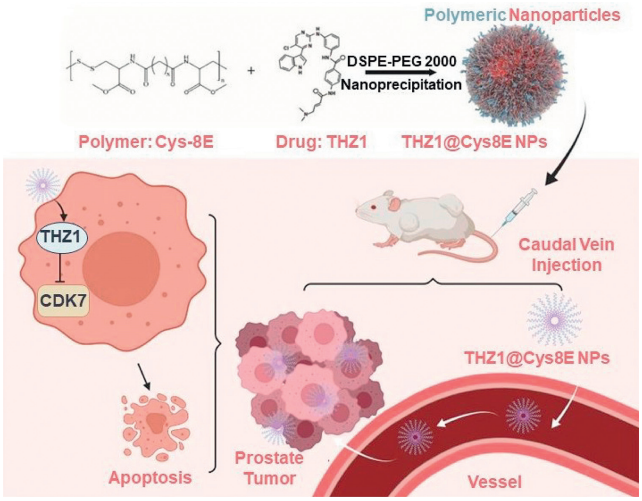

Scheme 1. Illustration of the procedures including synthesis route of THZ1@Cys8E NPs and it induces PCa cells apoptosis *via* vein injection. In the tumor environment, upon the stimulation of high level GSH, THZ1@Cys8E NPs releases drugs and inhibits CDK7 to work as a treatment in PCa.

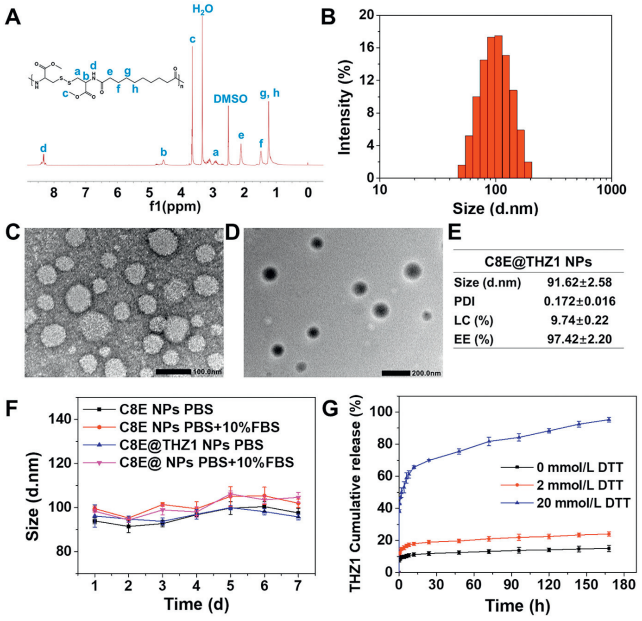

Fig. 1. Characteristics of the C8E and C8E@THZ1. (A) ^{1}H NMR spectrum of C8E NPs. (B) Size distribution of C8E@THZ1. (C) The representative TEM image of C8E@THZ1. (D) The typical TEM image of C8E NPs. (E) The average size and PDI of C8E@THZ1. (F) Stability of C8E NPs and C8E@THZ1. (G) Cumulative release of THZ1 in C8E@THZ1.

exceeded 90%, however, under PBS or 2 mmol/L DTT conditions was less than 20%, demonstrating that THZ1 can be effectively released within the tumor microenvironment (Fig. 1G). The above results suggested that we had successfully prepared nano-delivery carriers that are stable under physiological conditions and have excellent reduction responsiveness within the tumor.

After the successful preparation of the nanoparticles, we gave the attention on the intracellular paths of nanoparticles which were important for their function. Then we observed the cellular uptake and intracellular distribution of C8E NPs through a fluorescent probe, coumarin 6. Compared with free coumarin 6, the loading of C8E NPs enhanced the uptake of fluorescent probes in 22RV1 cells, and the results of fluorescence images and flow cytometry both showed that the uptake of nanoparticles was time depen-

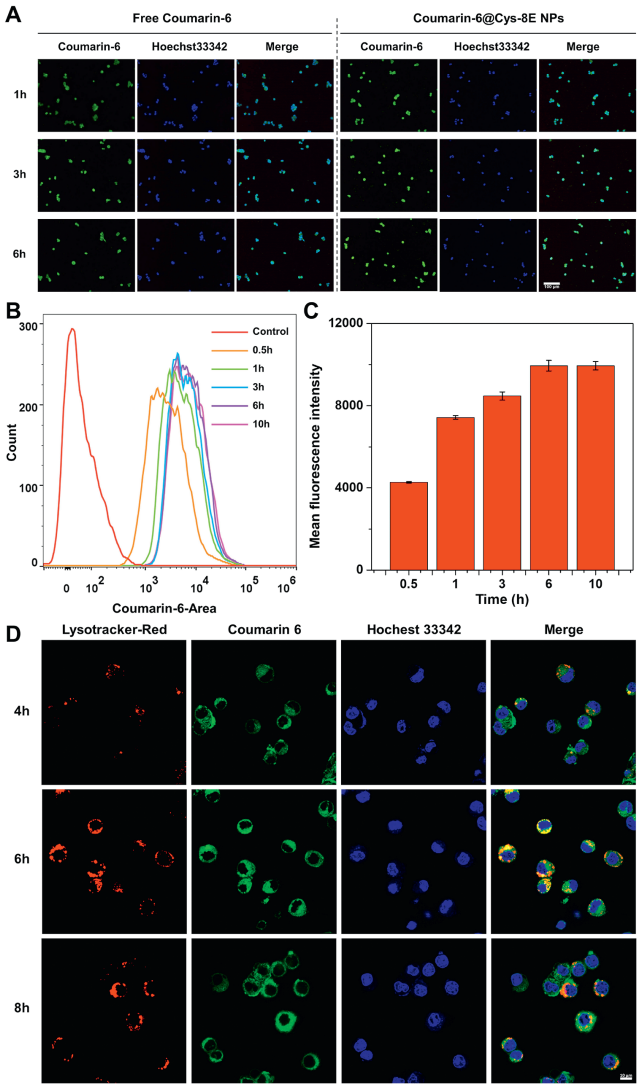

Fig. 2. Uptake and biodistribution of C8E NPs *in vitro*. (A) Cellular uptake images of PCa cells lived with coumarin 6@C8E NPs and free coumarin 6. Scale bar: 100 μm. (B, C) The cellular uptake result analysis of PCa cells after living with coumarin 6@C8E NPs by the flow cytometry. $n = 3$, mean ± standard deviation (SD). (D) Distribution of the coumarin 6@C8E NPs in PCa cells at different times. Scale bar: 10 μm.

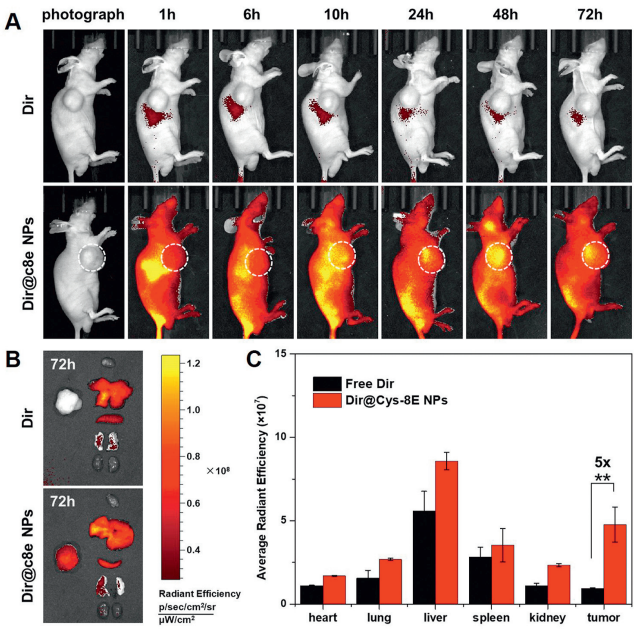

Fig. 3. The *in vivo* distributing track and tumor accumulation of C8E NPs. (A) Distributing track of the DIR and DIR@ C8E NPs in 22RV1 tumor-bearing mice. (B) Fluorescence signal images of tumors and major organs at 72 h. (C) Quantitative analysis result of the fluorescence signal intensity of tumors and the major organs. $n = 3$, mean ± SD. $^{**}P < 0.01$. 5×: 5 fold.

dent (Figs. 2A–C). With time passing, after 6 h of incubation, the green fluorescence (coumarin 6) and red fluorescence (lysosomes) in 22Rv1 cells overlapped obviously, while the overlap decreased significantly after 8 h (Fig. 2D), indicating that the nanoparticles could effectively enter the cells and escape from the lysosomes to the cytoplasm.

Besides the cellular uptake and intracellular distribution of nanoparticles, the *in vivo* performance was worthy exploring. And 1,1-dioctadecyl-3,3,3,3-tetramethylindotricarbocyaine iodide (DIR) was usually used to ulteriorly evaluate the *in vivo* distribution and accumulation of nanoparticles with 22RV1 tumor-bearing mouse model. Free DIR or DIR@C8E NPs were respectively injected into the tumor-bearing mice intravenously, and then photographed by the IVIS imaging system. According to the fluorescence images at different times *in vivo* (Fig. 3A), here was more DIR@C8E NPs accumulating in the tumors and detained for a longer time. Meanwhile, the fluorescence intensity of the free DIR group was mainly concentrated in the liver and rarely accumulated in the tumors. It could be suggested that nanoparticles group have the potential to enhance inhibitor accumulation and lengthen its residence time in the 22RV1 tumors. At 72 h, the tumors and major organs in both groups were dissected for fluorescence imaging and quantification (Figs. 3B and C). Consistently, in comparison to free DIR group, the average fluorescence intensity of the DIR@C8E NPs group was markedly higher (about 5 times) in the tumors and was less in other organs.

The increased inhibition efficiency of THZ1 by nanocarrier was the focus that we needed to detect. We further investigated the efficacy of THZ1 with or without the help of C8E NPs, as a drug delivery system, in PCa cells (22RV1 and LNCaP). THZ1 and C8E@THZ1 both reduced PCa cells viability in a dose-dependent manner, and improved therapeutic efficacy of C8E@THZ1 with approximately one-fifth of the half maximal inhibitory concentration (IC_{50}) compared to free THZ1 (Figs. 4A and B, Table S1 in Supporting information). On the basis of the CCK8 experiments, 20 nmol/L was chosen as the therapeutic dose of THZ1 and C8E@THZ1 *in vitro*. With this dose of drug, CDK7 can be inhibited in prostate cancer cells (Fig. 4C).

We further verified the auxiliary inhibitory effect of C8E NPs on THZ1 *in vitro*. Firstly, we studied the inhibiting effect of C8E@THZ1 by cell proliferation experiment. As shown in Figs. 4D and E, both C8E@THZ1 and THZ1 could inhibit the proliferation of 22RV1 and LNCaP cells, meanwhile, the inhibiting effect of C8E@THZ1 is stronger than THZ1. Similar results were obtained in the plate clone formation experiment of 22RV1 cells. Compared with the control group, C8E@THZ1 and THZ1 could inhibit the 22RV1 cell clone formation, besides, C8E@THZ1 had better inhibiting capability (Figs. 4F and G). To go further, apoptosis assays were conducted to show that C8E@THZ1 and THZ1 could facilitate the apoptosis of 22RV1 and LNCaP cells in comparison to the control group and a more than 25% apoptosis rate was exceeded in the C8E@THZ1 group over the THZ1 group (Figs. 4H–J). The above results confirmed that C8E@THZ1 might inhibit the proliferation and augment the *in vitro* apoptosis of prostate cancer cells, and performed better capability than free THZ1. Subsequently, here were other *in vitro* typical functional experiments in 22RV1 cells to investi-

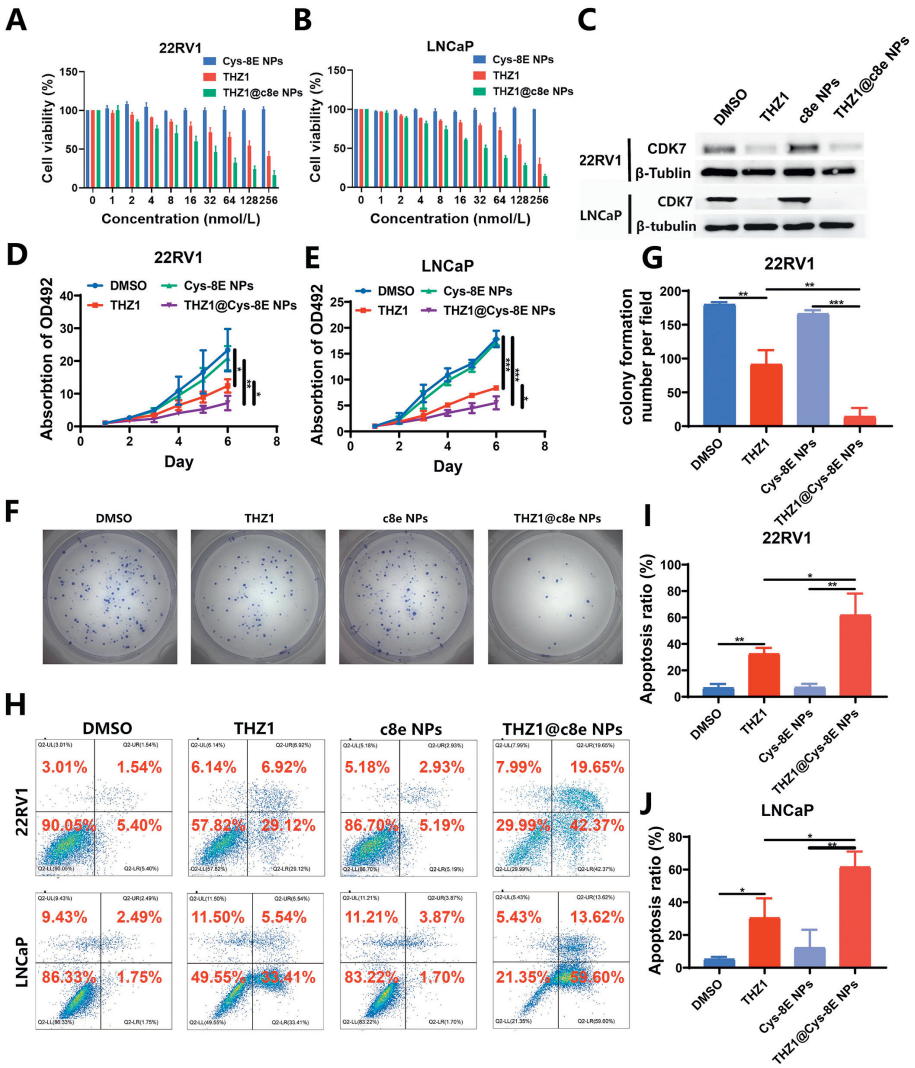

Fig. 4. Enhanced therapeutic efficacy caused by C8E@THZ1 *in vitro*. (A, B) 22RV-1 and LNCaP viability after incubation with THZ1, C8E NPs and C8E@THZ1. (C) The expression of CDK7 in 22RV-1 and LNCaP cells cultured with DMSO, THZ1, C8E NPs and C8E@THZ1. (D, E) The cell proliferation experiments of 22RV-1 and LNCaP cells. (F, G) Optical images and the corresponding quantitative analysis of 22RV1 cell clone formation experiments. (H–J) Optical images and quantitative analysis of apoptosis in 22RV1 and LNCaP cells by flow cytometry. $n = 3$, mean ± SD. $^{*}P < 0.05$, $^{**}P < 0.01$, $^{***}P < 0.001$.

gate thoroughly the function of C8E@THZ1. As shown in Figs. S1A and B (Supporting information), C8E@THZ1 and THZ1 did not induce 22RV1 cell cycle arrest *via* the cell cycle. Through cell migration and invasion experiments, compared with the control group, C8E@THZ1 and THZ1 both could suppress the migrating and invading behaviors of 22RV1 cells, but here was no significant distinction between them (Figs. S1C–E in Supporting information). However, the inhibitory effects of C8E@THZ1 and THZ1 on the migration and invasion of 22RV1 may be more related to their promotion of apoptosis. Next, 3D cell spheroidization experiment was conducted to evaluate the effect of C8E@THZ1 and THZ1 on the stemness of 22RV1. The results demonstrated that the balling ability of 22RV1 could be inhibited by C8E@THZ1 and THZ1, but they were also not significantly different (Figs. S1F and G in Supporting information).

The *in vivo* experiments were closed to the clinical application. To verify the *in vivo* efficacy of the nanoparticles, the xenograft tumor mouse model was used for the anti-tumor experiment. All *in vivo* experiments on mice were reviewed and approved by the Ethics Boards and the Clinical Research Committee at Sun Yat-sen University. The animals used in this study was approved by the Institutional Animal Care and Use Committee, Sun Yat-sen University (No. 2021000024). Xenografts bearing mice were randomly fixed up to four groups ($n = 5$) and injected with PBS, THZ1 (10 mg/kg, once every two days), C8E NPs (an equivalent amount of group C8E@THZ1) and C8E@THZ1 (10 mg/kg, once every two days) for 30 days. It was showed that the weight gain of group C8E@THZ1 and group THZ1 were more than the control group, and that of group C8E@THZ1 was more than group THZ1 (Fig. 5A). Moreover, C8E@THZ1 and THZ1 obviously lessened the volume and weight of tumors, and C8E@THZ1 had a much preferable curative effect than THZ1 and up to 85% (Figs. 5B–D). In addition, as shown in hematoxylin-eosin (HE) staining, the vascular density in group C8E@THZ1 and THZ1 were lower than that in the control group (Fig. 5E). These above results confirmed that here was stronger *in vivo* inhibitory effect of C8E@THZ1 than that of THZ1 on prostate cancer.

In the foregoing experiments, it was demonstrated that THZ1 could facilitate the apoptosis process of PCa cells, but its adverse reactions cannot be ignored in clinical application. Next, we probed into the influence of C8E NPs on reducing side effects of THZ1. *Via* observing HE staining results of the main organs of the above groups, there was no obvious histological damage in every group (Fig. 5F). Moreover, the blood biochemical results of mice in the

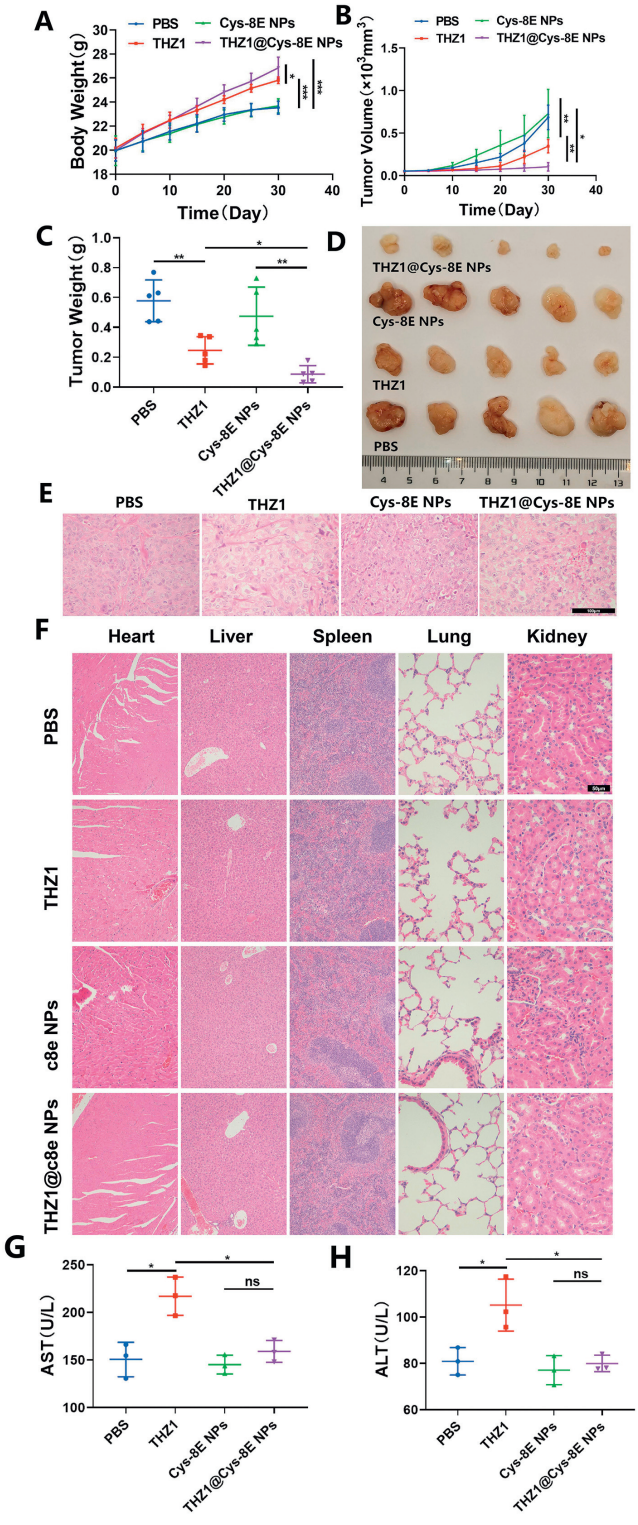

Fig. 5. Enhanced therapeutic efficacy caused by C8E@THZ1 *in vivo*. (A) The body weight changes of 22RV1 tumor-bearing mice. (B, C) Tumors volume and weight of tumor-bearing mice with different treatments. (D) Images of tumors among four groups including control, THZ1, C8E NPs and C8E@THZ1. (E) HE staining of tumors. Scale bar: 100 μm. (F) HE staining of hearts, livers, spleens, lungs and kidneys from four groups mice. Scale bar: 50 μm. (G, H) AST and ALT analysis results. $n = 5$, mean ± SD. One-way analysis and unpaired student's *t*-test. ns: not significant. $^{*}P < 0.05$, $^{**}P < 0.01$, $^{***}P < 0.001$.

above groups showed that there was a obvious increased of alanine aminotransferase (ALT) and azelaic aminotransferase (AST) in the THZ1 group, which indicated that THZ1 might cause liver function impairment in mice. And there was no significant change in the relevant indexes in the C8E group and the C8E@THZ1 group (Figs. 5G and H). Besides, there was no significant discrepancy in each group in every group on urea nitrogen (BUN) and creatinine (CR) (Fig. S2 in Supporting information). The above results indicated that the C8E system possesses a high level of safety and can effectively minimize the toxic side effects of the drug.

PCa is one of serious public health problems and results in a lot of deaths among male worldwide [10]. AR works as a vital driver in prostate carcinogenesis, and inhibitors of AR, abiraterone, darolutamide, enzalutamide, and apalutamide could improve outcomes and become a traditional primary treatment in PCa [11]. However, responses to these drugs are frequently not durable for the means of building resistance to them include AR amplification and mutation, and novel emerging mechanisms in compensatory steroid hormone such as estrogen receptor or glucocorticoid receptor [4].

As CDK7 inhibition could impair the function of AR through MED1 inactivation, it was suggested that CDK7-directed therapy might become an effective method against AR resistance mechanisms. Moreover, the novel CDK7 substrate MED1 T1457 is essential for promoting AR-mediated transcription, making CDK7 a potential therapeutic target in advanced prostate cancer. Then CDK7-specific inhibitors could act as monotherapy or work in refractory CRPC combined with second-generation antiandrogens [6]. As a specific covalent inhibitor of CDK7, THZ1 could suppress cancer cell growth and induce apoptosis *via* inhibiting the transcription of super-enhancer-associated oncogenes selectively [12].

Due to the EPR effect and great biocompatibility of the nanoparticles, loaded drug nanoplatform could enhance the function drug in impairing tumor growth in more safety in comparison to free drug [13,14]. Furthermore, we prepared THZ1 nanocarrier with hydrophobic cysteine-based poly(disulfide amide) (Cys-PDSA) polymers. These nanoparticles could respond to GSH *via* disulfide-mediated reduction so that loaded agent might be mostly released from the nanocarrier in tumor environment meanwhile fractionally released in the normal tissues [15,16].

In this study, with greater drug loading and more accurate delivery, C8E@THZ1 reduced toxicity and enhanced the antitumor effect of THZ1, that made it possible for clinical application of THZ1 in PCa.

Declaration of competing interest

The authors declare that they have no known competing financial interests or personal relationships that could have appeared to influence the work reported in this paper.

Acknowledgments

This work was supported by the National Key R&D Plan of China (No. 2022YFC3602904); the National Natural Science Foundation of China (Nos. 81974395, 82173036); Guangdong Basic and Applied Basic Research Foundation (No. 2019A1515011437); International Science and Technology Cooperation Project Plan of Guangdong Province (No. 2021A0505030085); Sun Yat-Sen University Clinical Research 5010 Program (No. 2019005); Beijing Bethune Charitable Foundation (No. mnzl202001); Guangzhou Science and Technology Key R&D Project (No. 202206010117); Beijing CSCO Clinical Oncology Research Foundation (Nos. Y-tongshu2021/ms-0162, Y-MSDZD2022-0760); Guangdong Province Key Laboratory of Malignant Tumor Epigenetics and Gene Regulation (No. 2020B1212060018OF006); Guangdong Provincial Clinical Research Center for Urological Diseases (No. 2020B1111170006);

Supported by the Open Research Funds from the Sixth Affiliated Hospital of Guangzhou Medical University, Qingyuan People's Hospital to Hai Huang.

This study was supported by the National Natural Science Foundation of China (Nos. 52173150, 51973243), the Open Research Funds from the Sixth Affiliated Hospital of Guangzhou Medical University, Qingyuan People's Hospital to Jun Wu.

This study was supported by the National Natural Science Foundation of China (No. 82173088), Natural Science Foundation of Guangdong (No. 2022A1515012383), the Guangzhou Science and Technology Fund (No. A202201011299), Baiqiuen Fund to Kaiwen Li. Fundamental Research Funds for the Central Universities, Sun Yat-sen University to Kaiwen Li.

Supplementary materials

Supplementary material associated with this article can be found, in the online version, at doi:10.1016/j.cclet.2023.109170.

References

[1] R.J. Rebello, C. Oing, K.E. Knudsen, et al., Nat. Rev. Dis. Primers 7 (2021) 9.
[2] H. Li, Q. Wang, Cancer Pathog. Ther. 1 (2023) 216–219.
[3] B. Shree, K. Das, V. Sharma, Cancer Pathog. Ther. 1 (2023) 195–204.
[4] J.W. Russo, M. Nouri, S.P. Balk, Cancer Discov. 9 (2019) 1490–1492.
[5] Z. Xie, Q. Zhou, C. Qiu, et al., Cancer Pathog. Ther. 1 (2023) 127–140.
[6] R.U. Rasool, R. Natesan, Q. Deng, et al., Cancer Discov. 9 (2019) 1538–1555.
[7] H. Tian, T. Zhang, S. Qin, et al., J. Hematol. Oncol. 15 (2022) 132.
[8] Z. Li, J. Huang, T. Du, et al., Chin. Chem. Lett. 33 (2022) 2496–2500.
[9] R. Zhang, T. Nie, Y. Fang, et al., Biomacromolecules 23 (2022) 1–19.
[10] Y. Zhu, M. Mo, Y. Wei, et al., Nat. Rev. Urol. 18 (2021) 282–301.
[11] D. Westaby, M.L.D. Fenor de La Maza, A. Paschalis, et al., Annu. Rev. Pharmacol. Toxicol. 62 (2022) 131–153.
[12] M. Wong, Y. Sun, Z. Xi, et al., Nat. Commun. 10 (2019) 3319.
[13] J. He, C. Li, L. Ding, et al., Adv. Mater. 31 (2019) e1902409.
[14] R. Liu, C. Luo, Z. Pang, et al., Chin. Chem. Lett. 34 (2023) 107518.
[15] H. Chen, Z. Liu, B. Wei, et al., Bioact. Mater. 6 (2021) 655–665.
[16] Y. Yang, Y. Zhang, R. Wang, et al., Chin. Chem. Lett. 33 (2022) 4583–4586.